ISSN 0023-1584, Kinetics and Catalysis, 2008, Vol. 49, No. 4, pp. 537–544. © MAIK "Nauka/Interperiodica" (Russia), 2008.
Original Russian Text © S.N. Orlik, 2008, published in Kinetika i Kataliz, 2008, Vol. 49, No. 4, pp. 562–569.

III INTERNATIONAL CONFERENCE "CATALYSIS: FUNDAMENTALS AND APPLICATIONS"

Combined Effect of the Redox and Acid–Base Properties of Catalysts in Redox Conversions of Nitrogen Oxides and Methane

S. N. Orlik

Pisarzhevskii Institute of Physical Chemistry, National Academy of Sciences of Ukraine, Kiev, Ukraine
e-mail: orlyk@inphyschem-nas.kiev.ua

Received July 19, 2007

Abstract—The results of the development of the concept of the combined effect of the acid–base and redox properties of catalysts in the selective catalytic reduction of nitrogen oxides (NO, N_2O) by C_1–C_4 hydrocarbons, in the partial oxidation of C_2–C_3 hydrocarbons by nitrogen oxides (NO, N_2O), and in the carbon dioxide reforming and total oxidation of methane are presented.

DOI: 10.1134/S0023158408040137

The increased interest in heterogeneous catalytic oxidation reactions is due to the practical use of these processes in the industrial-scale synthesis of valuable products and in environmental catalysis. Until the 1960s–1970s, the oxygen–catalyst bond energy, i.e., the redox properties of the catalyst, was considered to be the parameter determining the catalytic activity in these reactions. In 1968, G.I. Golodets advanced the concept that the acid–base properties of catalysts play an important role in catalytic activity and selectivity in redox processes [1]. These concepts were developed and generalized in later studies [2, 3].

In the present work, we report the results of using these approaches in the design of catalysts and processes for the conversion of nitrogen oxides and methane, in particular, the selective catalytic reduction of nitrogen oxides (NO, N_2O) with C_1–C_4 hydrocarbons (SCR with HC), the partial oxidation of C_2–C_3 hydrocarbons with nitrogen oxides (NO, N_2O), and oxidative methane conversion (total oxidation and carbon dioxide reforming).

Reduction of nitrogen oxides (NO_x) with hydrocarbons. It was found for the selective catalytic reduction of NO by light hydrocarbons (CH_4, C_3H_6, C_3H_8–C_4H_{10}) in the presence of zirconium dioxide–supported catalysts M_xO_y/ZrO_2 (M = Co, Cr, and Ce) that catalytic activity depends on the acid properties of the surface (the strength and type of the acid sites). The results of studying the acid properties of the catalyst surface by temperature-programmed ammonia desorption (ammonia TPD) and IR spectroscopy (pyridine adsorption technique) showed that the most active SCR catalysts have strong Brønsted acid sites [4, 5].

The ZrO_2-based oxide catalysts were promoted with minor amounts of rhodium (0.5 wt %) to improve their catalytic properties in nitrogen monoxide conversion [6]. The activity of the promoted catalysts was somewhat higher, but the order of the activities of the Rh–M_xO_y/ZrO_2 catalysts (M = Co, Cr, and Ce) in the SCR of NO with a propane–butane (2 : 1) mixture remained unchanged (Cr > Co ⩾ Ce). The results of studying the rhodium-promoted catalysts by x-ray photoelectron spectroscopy (XPS) showed that the Cr^{3+}, Ce^{4+}, and Co^{2+} ions in the corresponding samples experience a noticeable electron-acceptor effect of ZrO_2 and the valence state of rhodium is unaffected (Rh(I) with its characteristic binding energy of 308.5 eV) [5, 7].

The acid properties of the sample surface were studied by IR spectroscopy (pyridine adsorption technique) and ammonia TPD to understand why the activities of the rhodium-promoted oxide catalysts (chromium–zirconium and cerium–zirconium) are different [8]. In the case of Rh–Cr_2O_3/ZrO_2, the absorption bands characteristic of the pyridinium ion (1637 and 1545 cm^{-1}) appear in the IR spectrum, indicating that Brønsted acid sites are present on the sample surface. The observed absorption bands (1620, 1490, and 1440 cm^{-1}) indicate the formation of adsorption complexes between pyridine and electron-withdrawing catalyst sites [9]. No absorption bands are observed in this region for the Rh–CeO_2/ZrO_2 sample. This possibly indicates that the number of acidic functional groups on the surface of this catalyst is considerably smaller. The results of studying the acidity of the catalyst surface by IR spectroscopy and ammonia TPD are consistent. The more active catalyst Rh–Cr_2O_3/ZrO_2 contains strong ***B***-sites [5, 8].

As was found by IR spectroscopy, the adsorption and coadsorption of the reactants (NO, C_3H_6) differ substantially, depending on the nature of the surface of the rhodium-doped M_xO_y/ZrO_2 oxide system. The absence of acidic functional groups on the Rh–

Table 1. SCR activity of the cobalt-containing (10 wt % CoO) catalysts supported on ZrO_2*

Catalyst	NO conversion, %/*T*, °C**	
	$(C_3H_8–C_4H_{10}) + NO + O_2$	$CH_4 + NO + O_2$
$Rh–CoO/ZrO_2$	51/300	41/300
CoO/ZrO_2	40/300	72/300
$CoO/SO_4^{2-}/ZrO_2$	–	26/360
$CoO(Mn, Fe)/SO_4^{2-}/ZrO_2$	–	62/350

* The mixture contains 0.05% NO, 0.09% C_nH_m, 5% O_2, and the rest is Ar; $V = 6000\ h^{-1}$.
** The temperature at which the indicated conversion was achieved.

CeO_2/ZrO_2 surface [10] considerably decreases the activity of this catalyst in the selective reduction of NO with propene.

The rhodium-promoted cobalt–zirconium catalyst shows a lower SCR activity in methane reduction than the unpromoted sample (Table 1) [7]. For the SCR of NO with methane on the cobalt-containing catalyst, the active sites are protons of the support and Co^{2+} ions, on which the following steps of the process occur [11]:

$$\text{on } Co^{2+}: \quad NO + O_2 \Rightarrow NO_2,$$

$$\text{on } H^+: \quad 2NO_2 + CH_4 \Rightarrow CO_2 + 2H_2O + N_2.$$

Several possible routes for nitrogen formation on the protonated sites of the support have been discussed in the literature. According to some views, adsorbed NO_2 reacts with a hydrocarbon molecule to form a nitroalkane, which then yields molecular nitrogen. The importance of nitromethane and nitrosoalkane as intermediates formed in the reaction of hydrocarbon with adsorbed NO_2 was assumed by several researchers (see [11]). Another possibility is the protonation of CH_4 by a Brønsted acid site resulting in the intermediate carbocation CH_5^+, which is then attacked by NO_2 from the gas phase. Thus, the oxidation of NO to NO_2 and the reduction of NO_2 to N_2 occur on a combination of acid (H^+) and cationic sites. The necessity of dual sites combining different functions reflects the nature of the SCR process [7, 12].

Other ways of activating the reactants (NO and CH_4) appear when rhodium is introduced into the CoO/ZrO_2 catalyst. Nitrogen oxide can interact with Rh via the following scheme [13]:

$$NO + Rh^0 \Leftrightarrow Rh^+NO^- \xrightarrow{Rh^0} Rh^0–N + Rh^0–O$$

$$Rh^+NO^- \xrightarrow{2Rh^0} (Rh^+)_2O^{2-} + Rh^0–N.$$

Adsorbed oxygen decreases the free catalyst surface area accessible to NO_x, decreasing the efficiency of the conversion of the nitrogen oxides. The retardation of the reaction in excess oxygen can be caused by the competitive adsorption of NO and O_2 on the same rhodium active sites and by the competition between the oxidants (NO and O_2) for the hydrocarbon as the reducing agent. The role of the reducing agent (methane) is to remove adsorbed oxygen and to reduce the catalyst (rhodium active site).

The cleavage of the C–H bond in the methane molecule is the rate-determining step of NO reduction by methane on Rh/Al_2O_3 [14]:

$$CH_4 \Rightarrow CH_{3,ads} + H_{ads}.$$

Thus, the decreased nitrogen monoxide conversion in selective reduction by methane on $Rh–CoO/ZrO_2$ as compared to the unpromoted CoO/ZrO_2 sample can be explained by the activation of the reactants (NO and CH_4) via other routes, which are energetically and kinetically less favorable than the steps of NO and CH_4 conversion on cobalt oxide and on the proton site of the support (***B***-site of ZrO_2 modified by transition metal oxides).

The results obtained show that the enhancement of the redox properties of the M_xO_y/ZrO_2 catalysts due to the introduction of rhodium did not change their bifunctional nature and confirmed the importance of catalyst bifunctionality (the presence of redox sites and strong Brønsted acid sites) for the manifestation of the SCR activity [12].

Sulfated zirconia (as a solid superacid) attracts researchers' attention due to its low sensitivity to water vapor and sulfur dioxide and the high regenerating ability of the catalysts after SO_2 removal from the reaction mixture, which is particularly important for gas purification catalysts. Under the conditions of NO SCR with methane, cobalt-containing catalysts based on sulfated zirconia manifest a lower activity than the nonsulfated samples, which are characterized, according to IR spectroscopic data, by a higher concentration of surface ***B***-sites. The introduction of iron and manganese improves the catalytic properties of the sulfated system by increasing the concentration of active sites (the total concentration of acid and redox sites) (Table 1) [15, 16].

Conversion of nitrous oxide N_2O. The special attention given to N_2O conversion in the 21st century is due to the fact that, in the last decade, N_2O emissions into the atmosphere have increased 3–4 times more than methane emissions [17, 18]. An analysis of the molecular structure of N_2O (according to the proposed basicity scale, the proton affinity of nitrous oxide (576 kJ/mol) is comparable with those of methane (544 kJ/mol) and CO (593 kJ/mol)) suggests that N_2O is a Brønsted base [19]. In this connection, the character of N_2O activation can depend on the acid properties of the catalyst surface. The ***B***-sites of zeolites are capable of protonating the N_2O molecule: $N_2O + H^+ = {}^+N{=}N–OH$.

Table 2. Activity of the iron-containing catalysts in the decomposition and reduction of N_2O with a propane–butane mixture and carbon monoxide*

Catalyst	N_2O conversion, (T, °C)**				
	$N_2O + 1/2O_2$	$N_2O + (C_3H_8 + C_4H_{10})$	$N_2O + (C_3H_8 + C_4H_{10}) + O_2$	$N_2O + CO$	$N_2O + CO + O_2$
FeZSM-5***	95/550	93/400	93/450	92/450	83/560
Fe_2O_3/HZSM-5****	96/550	93/400	92/400	96/455	91/550
Fe_2O_3/HM	94/550	94/450	94/500	96/470	80/550
Fe_2O_3/[$(ZrO)^{2+}$–HZSM-5]	90/550	93/410	90/450	95/460	91/550
Fe_2O_3/[$(ZrO)^{2+}$–HMor]	86/550	91/450	91/500	94/460	91/550
Fe_2O_3/[$(ZrO)^{2+}$–HY]	15/550	91/490	57/550	94/525	24/550
Fe_2O_3/(35% ZrO_2 + 65% HZSM-5)	94/582	93/420	90/505	95/450	89/550

* The mixture contains 0.5% N_2O, 0.2% ($C_3H_8 + C_4H_{10}$) (2 : 1), 0.5% CO, 5% O_2, and He; $V = 6000\ h^{-1}$.
** The temperature at which the indicated conversion is achieved.
*** The degree of ion exchange is 93%.
**** The supported catalysts contain 10 wt % Fe_2O_3.

For this reason, catalysts with an acidic surface, namely, Fe-containing H-forms of zeolites of various structural types (faujasite (Y), mordenite (Mor), and pentasil (ZSM-5)) and ZrO_2 were studied in nitrous oxide conversion. In the direct decomposition of N_2O on the most active zeolite-based catalysts, which are characterized by the presence of strong acid sites on the surface (according to ammonia TPD data), 86–96% N_2O conversion is achieved at 500–550°C and gas flow rates of $(6–12) \times 10^3\ h^{-1}$ [20].

The data characterizing the reduction of N_2O by a propane–butane mixture and CO are presented in Table 2 and in Fig. 1. It can be seen that reduction by CO on the iron-containing catalysts occurs at temperatures close to the propane–butane reduction temperature; however, the temperature at which high N_2O conversions (92–96%) are achieved is 30–50 K higher than the temperature of reduction by C_3–C_4 hydrocarbons. In the presence of oxygen, N_2O is reduced by carbon monoxide at temperatures almost 100 K higher than in the absence of O_2 and 50–150 K higher than the temperature of SCR by C_3–C_4 hydrocarbons [21, 22].

The different catalytic activities of iron-containing zeolites of different structural types in N_2O reduction can be due to different conditions of reactant activation. As was mentioned above, N_2O can be activated on the ***B***-sites of zeolites. The activity of the Fe-containing pentasils in N_2O conversion is also attributed to the presence of ***α***-sites. Surface oxygen atoms and the acid–base sites of the catalyst are considered to participate in alkane activation [24]. The temperature of N_2O conversion upon the addition of a reducing agent

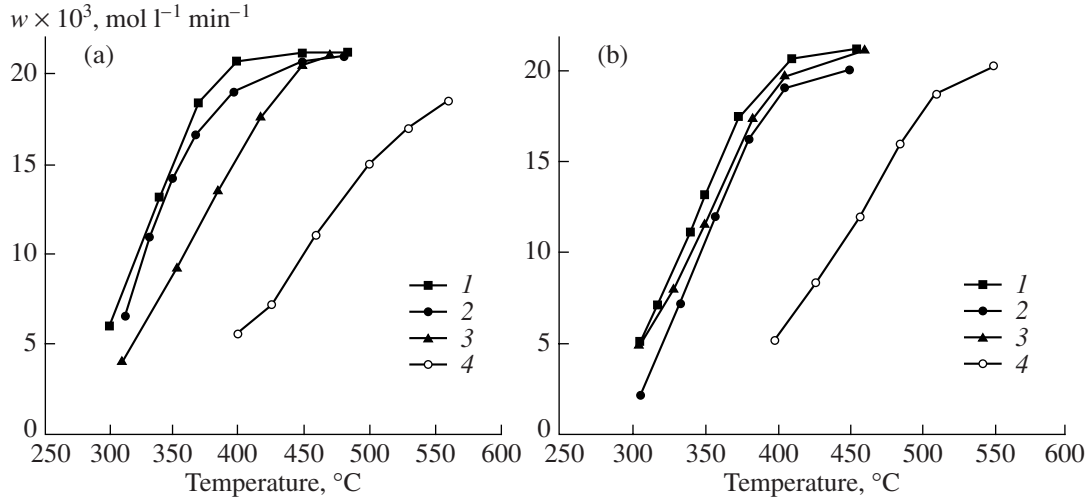

Fig. 1. Temperature dependence of the rate of N_2O conversion into nitrogen on the catalysts (a) FeZSM-5 and (b) Fe_2O_3/[$(ZrO)^{2+}$-HZSM-5] in the reaction mixtures (*1*) 0.5% N_2O–0.2% ($C_3H_8 + C_4H_{10}$) (2 : 1), (*2*) 0.5% N_2O–0.2% ($C_3H_8 + C_4H_{10}$) (2 : 1)–5% O_2, (*3*) 0.5% N_2O–0.5% CO, and (*4*) 0.5% N_2O–5% O_2; $V = 6000\ h^{-1}$.

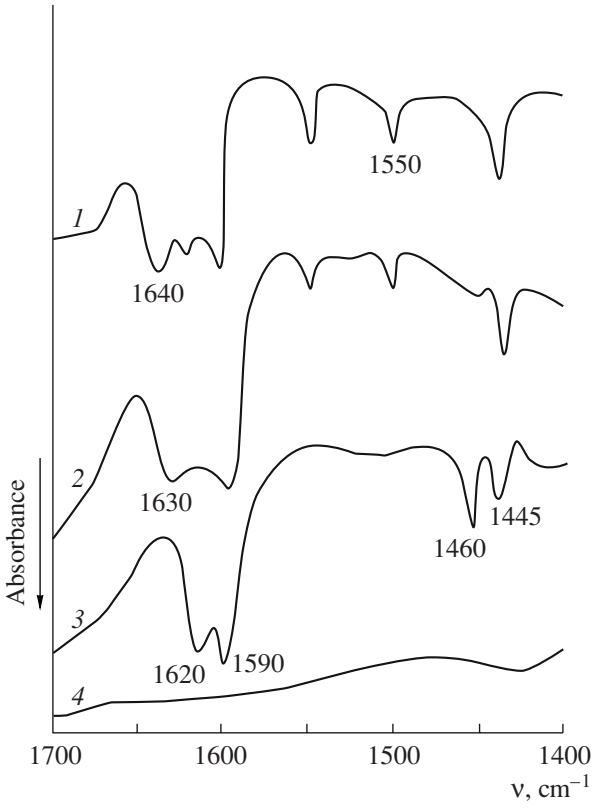

Fig. 2. IR spectra of the samples after pyridine adsorption: (*1*) Fe_2O_3/(35% ZrO_2 + 65% HZSM-5), (*2*) Fe_2O_3/[$(ZrO)^{2+}$–HZSM-5], (*3*) Fe_2O_3/[$(ZrO)^{2+}$-HY], and (*4*) the background spectrum of the catalyst before pyridine adsorption.

(a light alkane or CO) is 100–150 K lower than the temperature of the direct decomposition of nitrous oxide (Table 2). This can be due to the removal of oxygen formed by the associative adsorption of nitrous oxide on the catalyst [25].

The high (90–94%) N_2O conversions achieved at lower temperatures (400–450°C) under the conditions of SCR by hydrocarbons can be explained using mechanistic data on N_2O decomposition. This process has been the subject of a series of publications, most of which deal with N_2O decomposition on FeZSM-5 [25]. In the general case, the reaction $2N_2O \longrightarrow 2N_2 + O_2$ ($\Delta H^0_{r298} = -163$ kJ/mol) can be presented as the oxidation of the active sites ($N_2O + Z \longrightarrow N_2 + ZO$) followed by surface oxygen removal directly by the N_2O molecule itself ($N_2O + ZO \longrightarrow N_2 + O_2 + Z$), via the recombination of oxygen atoms ($2ZO \longrightarrow O_2 + 2Z$), or through the action of a reducing agent ($R + ZO \longrightarrow Z + RO$).

The process in an excess of the oxidant (under the SCR conditions) can be represented by the following simplified two-path mechanism:

$$(1)\ N_2O + Z \longrightarrow N_2 + ZO,$$
$$(2)\ N_2O + ZO \longrightarrow N_2 + O_2 + Z,$$
$$(3)\ O_2 + 2Z \longleftrightarrow 2ZO,$$
$$(4)\ R + Z \longleftrightarrow ZR,$$
$$(5)\ ZR + ZO \quad 2Z + RO,$$
$$N_2O + R = N_2 + RO,$$
$$2R + O_2 = 2RO,$$

where Z is the active site and R is the reducing agent ($C_3H_8 + C_4H_{10}$ or CO).

A more detailed scheme of the mechanism can include the impact interaction between the reducing agent and the oxidized site ($CO + ZO = CO_2 + Z$) and the activation of the hydrocarbon reductant on the acid sites of the zeolite catalyst, for example, through the formation of weak hydrogen bonds with the ***B***-acid sites (Si(OH)Al groups). In this case, the bond strength of adsorbed alkanes depends on the hydrocarbon chain length [26].

To elucidate the nature of the acid sites, particular catalyst samples were studied by IR spectroscopy using pyridine as the probe molecule. The IR spectra of pyridine sorbed on dehydrated samples are shown in Fig. 2. It is seen that the spectra contain absorption bands of the pyridinium ion (1550, 1620, 1630, and 1640 cm^{-1}), indicating that the Brønsted proton acid sites are present on the surface. Thus, the most active catalyst of the SCR of N_2O has strong ***B***-acid sites (a less active HY-based sample has weak ***L***- and ***B***-sites) [27]. The positive effect of the acidity of Pd–HZSM-5 on the reduction rate of $NO + N_2O$ by propene was observed [28].

Under the conditions of the N_2O SCR HC, high nitrous oxide conversions of 90–94% are achieved at temperatures 50–150 K lower due to the activation of the reducing hydrocarbon on the strong ***B***-sites, particularly the proton (H^+) sites of the zeolites and zirconium dioxide modified by transition metal oxides, followed by the interaction between the activated hydrocarbon and adsorbed atomic oxygen formed from N_2O or O_2:

$$C_nH_{2n+2} \overset{H^+}{\Rightarrow} (C_nH_{2n+3})^+ + O_{ads} \Rightarrow CO_x + H_2O.$$

Thus, the SCR activity of the oxide catalysts based on ZrO_2 and zeolites in NO and N_2O reduction depends on both the chemical nature and the strength of the redox and acid sites [29].

Partial oxidation of C_3–C_4 alkanes. The relationship between the acid properties of the surface and the catalytic activity in the selective oxidation of alkanes was found earlier [30, 31] and is observed for the partial oxidation of propane by nitrogen oxides (NO, N_2O) on catalysts of various types. For the partial oxidation of C_3–C_4 by nitrogen oxides (NO, N_2O) on zirconium dioxide modified by various heteropoly acids (HPAs), the catalytic activity depends on the amount of intro-

duced P–Mo HPA and the reaction selectivity with respect to the partial oxidation products changes in parallel with the concentration of weak acid sites [32].

In the partial oxidation of propane with N_2O into oxygen-containing compounds in the presence of the mesoporous material (Fe, Al)–MCM-41, the maximum yield of the major product (isopropanol) is one order of magnitude higher than the yields of the other oxygen-containing products. An analysis of XRD, IR, XPS, and NMR data for (Fe, Al)–MCM-41 makes it possible to attribute the high isopropanol yield to the activation of propane on the acid sites and to the activation of N_2O on the redox iron sites, due to which nitrous oxide acts as a mild oxidant to form isopropanol. Thus, a certain combination of the structural characteristics and acid and redox properties of the (Fe, Al)–MCM-41 surface provides catalytic activity in partial propane oxidation involving nitrogen(I) and nitrogen(II) oxides [33].

Selective oxidation of ethylene. The promoting effect of alkali metal admixtures on the target product yield was revealed in ethylene epoxidation by nitrous oxide on structured Ag-containing catalysts. The introduction of Cs, K, and Na microadmixtures raises the ethylene oxide yield by a factor of 1.5–2 due to the increase in selectivity with a decrease in the reaction onset temperature by 80–100 K [34]. The optimum alkali metal content (0.1–0.8 wt %) decreases in the order Na > K > Cs, which is antibatic to the corresponding order of atomic radii (Table 3). The key factor in achieving a promoting effect is the following sequence of introduction of the components: (1) M = Cs, K, Na; (2) Ag. For the opposite order, the deactivation of the catalyst is observed, which is evidently due to the blocking of the epoxidation active sites by the alkaline additives. Alkali metals substitute for, and thus reduce the concentration of, support protons [35], favoring subsequent ethylene oxide conversion to deep oxidation products. This conversion likely proceeds via isomerization into acetaldehyde on the acid sites.

Deep methane oxidation. A relation between the acid properties of the surface and catalytic activity is also observed in deep methane oxidation on nanodisperse complex oxide catalysts supported on porous Al_2O_3 and ZrO_2: the stronger the acid sites (according to ammonia TPD data), the lower the reaction onset temperature [36].

For supported nickel ferrites, the concentration of acid sites on Al_2O_3 is higher than that on the sample based on modified ZrO_2. The more active catalyst $NiFe_2O_4/(ZrO_2–Y_2O_3)$ has stronger acid sites ($T_{\max\ dec.NH_3}$ = 300°C) than $NiFe_2O_4/Al_2O_3$ ($T_{\max\ dec.NH_3}$ = 160°C). This is significant for the deep oxidation of hydrocarbons.

The most active Co–Zr catalysts, in which the total concentration of acid sites is low, have stronger acid sites. As a consequence, the onset temperature of deep methane oxidation on $Co_xO_y/(ZrO_2–HZSM\text{-}5)$ is lower than that on Co_xO_y/ZrO_2 (in both samples, ZrO_2 was prepared by sol–gel processing).

Table 3. Influence of the alkaline additives in the silver honeycomb catalysts on ethylene epoxidation with nitrous oxide

Catalyst (Ag, M_2O)/cordierite (M = Cs, K, Na)	Conversion of C_2H_4, %/T, °C	C_2H_4O	
		yield, %	selectivity, %
20% Ag	72/425	14	19
18% Ag, 0.5% Na	84/420	31	37
19% Ag, 0.8% Na	75/445	26	34
19% Ag, 1.5% Na	63/470	10	16
21% Ag, 0.1% K	85/410	30	35
18% Ag, 0.3% K	93/400	30	32
23% Ag, 0.7% K	79/415	28	36
19% Ag, 0.1% Cs	90/420	23	26
16% Ag, 0.3% Cs	73/415	20	27

Note: Composition of the mixture: 2% C_2H_4 + 60% N_2O; V = 90 $cm^3\ min^{-1}\ (g\ Cat)^{-1}$.

Among the supported oxide composites M_xO_y/ZrO_2 and M_xO_y/Al_2O_3, where M is Mn, Co, and Cr, Mn_xO_y/ZrO_2 exhibits the highest activity in deep methane oxidation (the temperature of 50% CH_4 conversion is T_{50} = 363°C). Hydrogen TPR and IR spectroscopic data indicate that the manganese–zirconium oxide composite is a bifunctional catalyst containing a greater amount of reactive oxygen, which activates the C–H bond more effectively than the Al_2O_3-based catalyst (Fig. 3). The activity of the supported manganese catalysts is determined by the support nature, the extent of dispersion of the manganese oxides, and the redox and acid properties. The most active low-temperature catalyst is characterized by an optimum combination of the size, redox, and acid characteristics [37]. Thus, the presence of strong acid sites on the catalyst surface is a factor ensuring the lower onset temperature of deep methane oxidation. The efficiency of the catalysts is determined by the strength of the oxygen–catalyst bond and by the acid properties of their surface. This is in good agreement with the modern mechanistic concepts of the deep oxidation of alkanes, including methane, on oxide catalysts.

Methane reforming with carbon dioxide (MRCD). The processes of oxidative methane reforming into synthesis gas are among the most important methods of the industrial-scale production of hydrogen and CO. Supported nickel catalysts are most active in the carbon dioxide reforming of methane, although they have a substantial drawback: they lose activity because of coking. The mechanism of the MRCD pro-

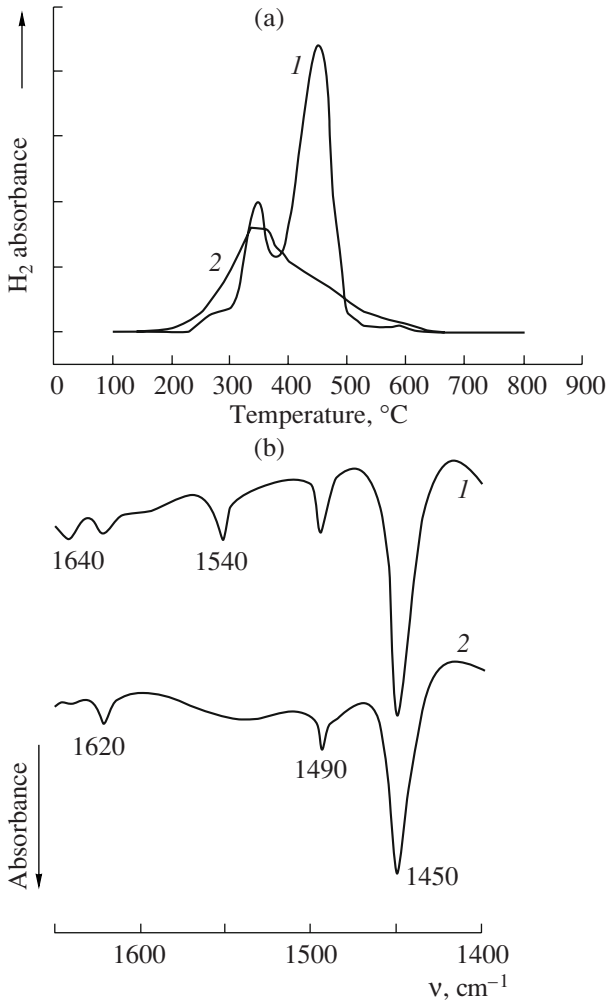

Fig. 3. (a) TPR curves and (b) IR spectra after pyridine adsorption on the catalysts (*1*) Mn_xO_y/ZrO_2 and (*2*) Mn_xO_y/Al_2O_3.

cess includes carbon formation as an intermediate step [38]:

$$CH_4 + Z \longleftrightarrow [CH_x]\text{–}Z + (4 - x)H_{ads} \longleftrightarrow ZC + 2H_2.$$

The activity of Ni-containing structured catalysts in the MRCD reaction depends on the conditions of active phase synthesis on the support surface. The catalytic activity is enhanced when the active phase (NiO) and the structure-forming component (Al_2O_3) are simultaneously supported on cordierite, which is due to the formation of structures of the nickel aluminate type at the heat treatment stage. These structures decompose during reduction into finely dispersed metallic nickel stabilized in the oxide–aluminum matrix.

The developed catalysts are not less active than the GIAP 3-6N commercial granulated catalyst, and their productivity far exceeds (by a factor of ≥2.5) the productivity of the latter owing to the higher accessibility of their catalytically active surface (Table 4).

The operating stability of the Ni-containing catalysts in MRCD can be enhanced by controlling the acid–base properties of their surface, particularly by the introduction of alkali metal oxides [39]. In this case, the basic oxide can substantially decrease the CH_4 conversion by suppressing the activated adsorption of methane and by stimulating the adsorption of the oxidant (CO_2), which can react with the surface carbon of the catalyst via the reverse Boudoir reaction

$$C + CO_2 = 2CO.$$

Therefore, the enhancement of the operating stability of the nickel–aluminum catalysts of the MRCD process can be attributed to the retardation of coke formation. The activity of the catalysts can be decreased by the formation of thermodynamically stable inactive alkali metal aluminates (Fig. 4a).

The study of the catalysts by hydrogen TPR showed that the reduction rate of $NiO–Al_2O_3$ binary systems, including the systems modified by additives of alkali metal oxides, changes in parallel with their activity in MRCD (Fig. 4b). An ammonia TPD study of the acid properties of the nickel catalysts showed that the modification by alkali metal or alkaline-earth metal oxides decreases the general acidity of the catalyst surface; i.e., an antibatic relationship is observed between the general acidity of the catalysts and the operating stability during the MRCD process. Thus, the enhancement of the stability of nickel-containing catalyst operation is due to a decrease in the general acidity of the surface [40].

Table 4. Activity and productivity of the nickel-containing catalysts in the carbon dioxide conversion of methane*

Catalyst	T_{80}, °C**	Productivity × 10^6,	
		mol s^{-1} (g Cat)$^{-1}$	mol s^{-1} (g NiO)$^{-1}$
GIAP-18, d = 1–2 mm	485	12.96	1.62
8.2% NiO/1.2% Al_2O_3/cordierite	487	38.3	4.8
3.8% NiO/11.2% Al_2O_3/cordierite	492	30.0	7.8
1% NiO/0.2% Al_2O_3/cordierite	533	27.6	27.6
GIAP-18, d = 15 × 15 mm	–	0.144	0.23

* Mixture composition, vol %: CH_4, 5.5; CO_2, 7.0; He, the rest; the flow rate of the reaction mixture was 6000 h^{-1} for the block catalysts and 3000 h^{-1} for the GIAP-18 samples.
** 80% CH_4 conversion temperature.

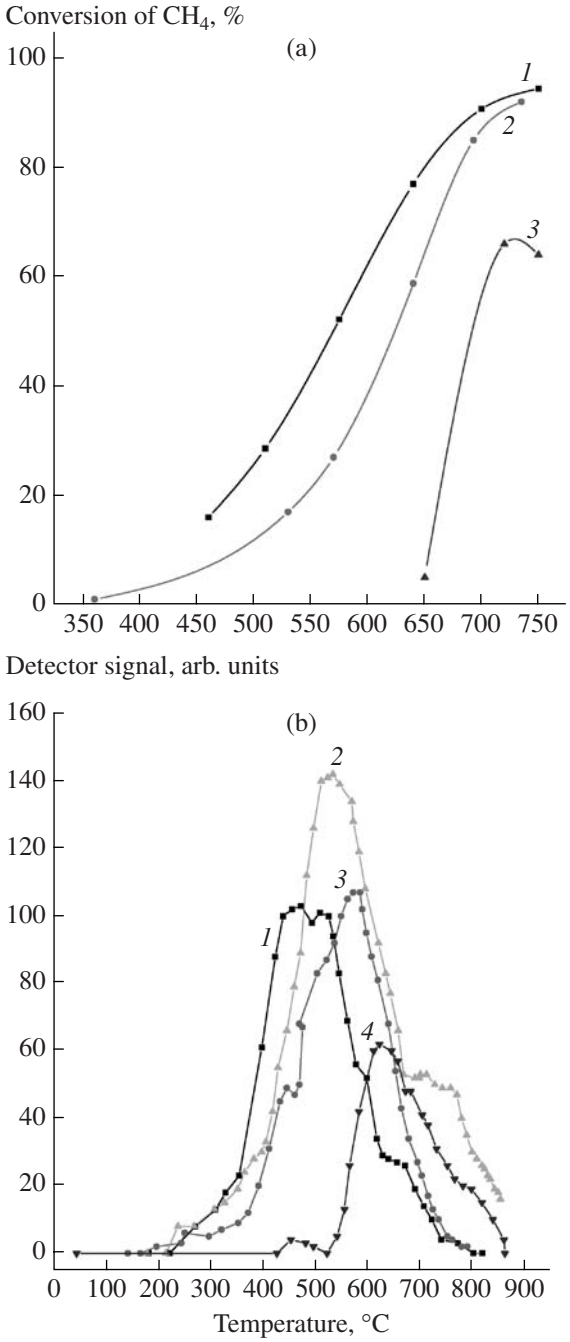

Fig. 4. (a) Temperature dependence of the carbon dioxide conversion of CH_4 (5.5 vol % CH_4, 7.0 vol % CO_2, the rest is He) in the presence of the catalysts (1% NiO + 0.2% Al_2O_3)/cordierite with additives of (*1*) 0.6% K_2O, (*2*) 0.9% Na_2O, and (*3*) 0.7% Li_2O; (b) temperature-programmed spectra of the catalyst (*1*) (1% NiO + 0.2% Al_2O_3)/cordierite with additives of (*2*) 0.6% K_2O, (*3*) 0.9% Na_2O, and (*4*) 0.7% Li_2O; (10% H_2/Ar, 50 cm^3/min, 10 K/min).

The results reported here are the development of the concept of the combined effect of the redox and acid–base properties of the catalyst in the redox processes. When selecting catalysts for these processes, it is necessary to consider the energy of the oxygen–catalyst bond and the acid–base properties of the surface. The bifunctional catalysts exhibit the highest activity and selectivity in nitrogen oxide (NO, N_2O) conversion. Due to the favorable combination of the redox and acid properties of their surface, the (Rh)–M_xO_y/ZrO_2 (M = Co, Cr, Ce) and Fe/H-zeolite (mordenite, faujasite, pentasil) catalysts exhibit high activity both in the selective reduction of nitrogen oxides into nitrogen and in the partial oxidation of light alkanes into oxygen-containing products. The modification of the surface of the silver catalysts supported on the honeycomb matrices of synthetic cordierite by alkali metals (Ag/(Cs, K, Na)/cordierite), i.e., the control of the acid–base properties of the surface, results in a promoting effect on the epoxidation of ethylene by nitrogen(I) oxide due to the increase in the selectivity of target product formation by 1.5–2 times. Methane activation during its deep oxidation at relatively low temperatures (280–350°C) is related to the presence of the reactive oxygen and strong acid sites on the surface of the complex oxide catalysts, in particular, the cobalt–zirconium and manganese–zirconium catalysts. The operating stability of the structured nickel catalysts in the carbon dioxide conversion of methane (NiO–Al_2O_3–(Li, Na, K)/cordierite) can be enhanced by controlling the acid–base properties of their surface.

REFERENCES

1. Golodets, G.I., *Dokl. Akad. Nauk SSSR*, 1969, vol. 184, p. 1334.
2. Golodets, G.I., *Heterogeneous Catalytic Reactions Involving Molecular Oxygen*, Amsterdam: Elsevier, 1983, p. 880.
3. Golodets, G.I., *Kinet. Katal.*, 1987, vol. 28, no. 1, p. 35.
4. Mironyuk, T.V., Struzhko, V.L., and Orlik, S.N., *Teor. Eksp. Khim.*, 2000, vol. 36, no. 5, p. 307.
5. Orlik, S.N., Struzhko, V.L., Mironyuk, T.V., and Tel'biz, G.M., *Kinet. Katal.*, 2003, vol. 44, no. 5, p. 744 [*Kinet. Catal.* (Engl. Transl.), vol. 44, no. 5, p. 682].
6. Orlik, S.M., Struzhko, V.L., and Mironyuk, T.V., *Ukr. Khim. Zh.*, 2002, vol. 68, no. 7, p. 32.
7. Orlik, S.N., Struzhko, V.L., Mironyuk, T.V., and Kazimirov, V.P., *Teor. Eksp. Khim.*, 2003, vol. 39, no. 3, p. 179.
8. Orlik, S.N., Struzhko, V.L., Mironyuk, T.V., and Tel'biz, G.M., *Teor. Eksp. Khim.*, 2001, vol. 37, no. 5, p. 306.
9. Little, L., *Infrared Spectra of Adsorbed Species*, London: Academic, 1966.
10. Struzhko, V.L., Mironyuk, T.V., Orlik, S.N., and Tel'biz, G.M., *Teor. Eksp. Khim.*, 2001, vol. 37, no. 6, p. 367.
11. Yan, J., Kung, M.C., Sachtler, W.M.H., et al., *J. Catal.*, 1998, vol. 175, no. 2, p. 294.
12. Mironyuk, T.V. and Orlyk, S.N., *Appl. Catal., B*, 2007, vol. 70, nos. 1–4, p. 58.

13. Chuang, S.S.C. and Tan, C.D., *J. Catal.*, 1998, vol. 173, no. 1, p. 95.
14. Hardee, J.R. and Hightower, J.W., *J. Catal.*, 1984, vol. 86, no. 1, p. 147.
15. Mironyuk, T.V., Struzhko, V.L., Orlik, S.N., and Tel'biz, G.M., *Teor. Eksp. Khim.*, 2005, vol. 41, no. 3, p. 121.
16. Mironyuk, T.V. and Orlyk, S.N., *Catal. Today*, 2007, vol. 119, nos. 1–4, p. 152.
17. Centi, G., Ciambelli, P., Perathoner, S., et al., *Catal. Today*, 2002, vol. 75, nos. 1–4, p. 3.
18. Leont'ev, A.V., Fomicheva, O.A., Proskurina, M.V., et al., *Usp. Khim.*, 2001, vol. 70, no. 2, p. 107.
19. Szulejko, J.E. and McMahon, T.B., *J. Am. Chem. Soc.*, 1993, vol. 115, no. 17, p. 7839.
20. Orlik, S.N., Ostapyuk, V.A., Pidruchna, T.M., and Struzhko, V.L., *Teor. Eksp. Khim.*, 2004, vol. 40, no. 3, p. 172.
21. Orlik, S.N. and Pidruchna, T.M., *Teor. Eksp. Khim.*, 2005, no. 1, p. 35.
22. Boichuk, T.M., Mironyuk, T.V., and Orlyk, S.M., *Pol. J. Environ. Stud.*, 2006, vol. 15, no. 6A, p. 11.
23. Kharitonov, A.S., Aleksandrova, T.N., Panov, G.I., et al., *Kinet. Katal.*, 1994, vol. 35, no. 2, p. 296.
24. Margolis, L.Ya. and Korchak, V.N., *Usp. Khim.*, 1998, vol. 67, no. 12, p. 1175.
25. Perez-Ramirez, J., Kapteijn, F., Mul, G., et al., *Catal. Today*, 2002, vol. 76, no. 1, p. 55.
26. Subbotina, I.R., Shelimov, B.N., and Kazanskii, V.B., *Kinet. Katal.*, 2002, vol. 43, no. 3, p. 445 [*Kinet. Catal.* (Engl. Transl.), vol. 43, no. 3, p. 412].
27. Orlyk, S.M., Mironyuk, T.V., and Boichuk, T.M., *Ads. Sci. Technol.*, 2007, vol. 25, no. 1, p. 23.
28. Izumi, Y., Kizaki, T., and Aika, K., *Bull. Chem. Soc. Jpn.*, 2001, vol. 74, no. 8, p. 1499.
29. Mironyuk, T.V., Boichuk, T.M., and Orlik, S.N., *Tezisy dokladov 7 Rossiskoi konferentsii "Mekhanizmy kataliticheskikh reaktsii"* (7th Russian Conf. on Mechanisms of Catalytic Reactions), St. Petersburg, 2006, part 1, p. 169.
30. Gomonai, V.I., in *Kataliz i katalizatory* (Catalysis and Catalysts), Kiev: Naukova Dumka, 1989, issue 26, p. 52.
31. Sokolovskii, V., *Catal. Today*, 1995, vol. 24, p. 377.
32. Orlik, S.N., Struzhko, V.L., Alekseenko, L.M., and Ostapyuk, V.A., *Teor. Eksp. Khim.*, 2002, vol. 38, no. 5, p. 304.
33. Orlik, S.N., Pop, G., Ganya, R., Ostapyuk, V.A., and Alekseenko, L.M., *Teor. Eksp. Khim.*, 2004, vol. 40, no. 3, p. 181.
34. Kapran, A.Yu. and Orlik, S.N., *Teor. Eksp. Khim.*, 2005, vol. 41, no. 6, p. 360.
35. Macleod, N., Keel, J.M., and Lambert, R.M., *Catal. Lett.*, 2003, vol. 86, nos. 1–3, p. 51.
36. Kantserova, M.R. and Orlik, S.N., *Kinet. Katal.*, 2007, vol. 48, no. 3, p. 438 [*Kinet. Catal.* (Engl. Transl.), vol. 48, no. 3, p. 414].
37. Kantserova, M.R., Orlik, S.N., and Kazimirov, V.P., *Teor. Eksp. Khim.*, 2007, vol. 43, no. 6, p. 367.
38. Krylov, O.V., *Ross. Khim. Zh.*, 2000, vol. 44, no. 1, p. 19.
39. Toshihiko, O. and Toshiaki, M., *J. Catal.*, 2001, vol. 204, no. 1, p. 89.
40. Solov'ev, S.A., Zatelepa, R.N., Gubareni, E.V., Strizhak, P.E., and Moroz, E.M., *Zh. Prikl. Khim.*, 2007, vol. 80, no. 11, p. 1883 [*Russ. J. Appl. Chem.* (Engl. Transl.), vol. 80, no. 11, p. 1883].